Cell surface–associated Tat modulates HIV-1 infection and spreading through a specific interaction with gp120 viral envelope protein

Serena Marchiò, Massimo Alfano, Luca Primo, Daniela Gramaglia, Luca Butini, Luisa Gennero, Enrico De Vivo, Wadih Arap, Mauro Giacca, Renata Pasqualini, and Federico Bussolino

Human immunodeficiency virus-1 (HIV-1) Tat, a nuclear transactivator of viral gene expression, has the unusual property of being released by infected cells. Recent studies suggest that extracellular Tat is partially sequestered by heparan sulfate proteoglycans. As a consequence, Tat is concentrated on the cell surface and protected from proteolytic degradation, thus remaining in a biologically active form. We show that Tat binds the surfaces of both HIV-1–infected and surrounding uninfected cells. We provide evidence for a specific interaction between Tat and the HIV-1 glycoprotein 120 (gp120) envelope protein, which enhances virus attachment and entry into cells. We map the interacting sites of both Tat and gp120 and show that synthetic peptides mimicking the gp120 site inhibit HIV-1 infection. Our data demonstrate that membrane-associated Tat is a novel modulator of virus entry and suggest that the Tat-gp120 interaction represents a critical step in HIV-1 spreading during the course of infection. (Blood. 2005;105:2802-2811)

Introduction

HIV-1 infection is characterized by early viremia followed by a long period of clinical latency[1-3] in which the level of virus production reflects a continuous process of new infection at a rate that balances the rapid death of productively infected cells (reviewed by Blankson et al[4]). After years, when a clinically apparent disease develops, this steady state is unbalanced toward an exponential increase in viral burden.[2] During all these steps, infected cells release soluble factors that likely contribute to the infectivity of nearby uninfected cells.[5]

The endogenous HIV-1 transactivator of transcription Tat, although known as a nuclear factor,[6] is released by infected cells both in vitro and in vivo[7-9] and seems to play several functions in the extracellular microenvironment. For example, a large number of results suggest that Tat could contribute to the onset of disorders associated with HIV-1 infection (ie, Kaposi sarcoma,[7,10] dementia,[11] lymphomas,[12] and kidney injury[13]).

Interestingly, a direct, nontranscriptional function of Tat in the setting of a spreading viral infection has also been suggested.[14-16] In accordance with this potential role of extracellular Tat, circulating anti-Tat antibodies (Abs) correlate with low or undetectable viral load in HIV-1–seropositive patients.[17-19] These observations are also confirmed by the ability of neutralizing anti-Tat Abs to reduce the viral load both in vitro and in vivo[20-22] (reviewed by Gallo[23] and Goldstein[24]). Despite the huge and often controversial scientific production regarding the role of extracellular Tat, an insight into the molecular mechanism(s) responsible for a Tat-driven spreading of infection remained so far elusive.

Here we demonstrate that membrane-bound Tat is a thus-far unrecognized mediator of HIV-1 entry. In particular, we show that Tat is present on the surface of HIV-1–infected and nearby uninfected cells, where it is specifically bound by HIV-1 gp120 envelope protein, leading to enhanced virus attachment and entry into cells. We also describe phage display–selected peptides that interfere with this binding, thus inhibiting HIV-1 entry and propagation of the infection.

Materials and methods

Reagents

The following reagents were provided through the European Union Program European Vaccine against AIDS/Medical Research Council (EVA/MRC), the Centralized Facility for Acquired Immunodeficiency Syndrome (AIDS) Reagents, and the National Institute for Biological Standards and Controls (Herts, United Kingdom): NT3 2D1 immunoglobulin G_1 (IgG_1) (donor, Dr J. Karn) and Sp2/0 (clone 20.1) IgM (donor, Dr K. Krohn) anti-Tat monoclonal Abs (mAbs); CRA3 IgG_{2a} anti-gp120 mAb (donor, Dr

From the Division of Molecular Angiogenesis and Division of Molecular Oncology, Department of Oncological Sciences, University of Turin Medical School, Institute for Cancer Research and Treatment, Candiolo, Italy; Creabilis Therapeutics, Colleretto Giacosa, Italy; AIDS Immunopathogenesis Unit, Department of Immunology and Infectious Diseases, San Raffaele Scientific Institute, Milan, Italy; Service of Clinical Immunology, Department of Internal Medicine, Marche Polytechnic University School of Medicine and Ancona General Hospital, Torrette di Ancona, Italy; Division of Infectious Diseases, Amedeo di Savoia Hospital, Turin, Italy; Service for Drug Addictions, Turin, Italy; The University of Texas MD Anderson Cancer Center, Houston, TX; and Molecular Medicine Laboratory, International Center for Genetic Engineering and Biotechnology, Trieste, Italy.

Submitted June 14, 2004; accepted November 17, 2004. Prepublished online as *Blood* First Edition Paper, December 9, 2004; DOI 10.1182/blood-2004-06-2212.

Supported by grants from Istituto Superiore di Sanità (AIDS projects) and Associazione Italiana per la Ricerca sul Cancro (AIRC).

Two of the authors (S.M. and F.B.) have a financial interest in a company (Creabilis Therapeutics, Colleretto Giacosa, Italy) whose potential products were studied in the present work.

Reprints: Serena Marchiò or Federico Bussolino, Institute for Cancer Research and Treatment, Department of Oncological Sciences, University of Turin School of Medicine, Sp 142, km 3.95-10060 Candiolo (TO) Italy; e-mail: serena.marchio@ircc.it; federico.bussolino@ircc.it.

The publication costs of this article were defrayed in part by page charge payment. Therefore, and solely to indicate this fact, this article is hereby marked "advertisement" in accordance with 18 U.S.C. section 1734.

M. Page); U937 and C8166 cells (donor, Dr G. Farrar); and recombinant Tat_{86} III B (rTat) and glycoprotein 120 (gp120) III B (rgp120; Immunodiagnostics, Woburn, MA). The following Tat variants from the laboratory-adapted strain HXB2 were produced as glutathione S-transferase (GST)–fused proteins as described[25]: Tat_{86} (product of Tat first and second exon), Tat_{72} (first exon), Tat_{Bas} (with the mutations R-49,52,53,55,56,57-A), and Tat_{Cys} (with the mutations C-22,25,27-A). The CSFNIT (CT303), RD-KVKK (CT304), CSFNITTEIRDKVKK (CT319), and GACVRLSACGA (control) peptides were from New England Peptide (Fitchburg, MA).

Cell cultures

U937, C8166, and MT4 (American Type Culture Collection [ATCC], LGC Promochem, Milan, Italy) cells were cultured in RPMI 1640 medium supplemented with 10% fetal calf serum (FCS); Phoenix cells (a gift from Dr Nolan, Stanford University, CA) were cultured in Dulbecco modified essential medium (DMEM) supplemented with 10% FCS; 293T cells (ATCC) were cultured in Iscove modified essential medium (IMDM) supplemented with 10% FCS. Peripheral blood mononuclear cells (PBMCs) from HIV-1–infected patients and the healthy donors were separated on a Ficoll-Hystopaque gradient and cultured in RPMI 1640 supplemented with 15% FCS and 200 U/mL interleukin-2 (IL-2; Chiron, Emeryville, CA). Patient samples were obtained following approval by the institutional review boards of the San Raffaele Scientific Institute in Milan, the Marche Polytechnic University in Ancona, and the Amedeo di Savoia Hospital in Turin; and written informed consent was obtained from all patients and healthy donors in accordance with the Declaration of Helsinki.

HIV-1–infected specimens

PBMCs from HIV-1–infected patients were frozen in FCS containing 10% dimethyl sulfoxide (DMSO) and stored in liquid nitrogen by the Service of Clinical Immunology (University of Ancona, Italy). Specimens from 20 patients were randomly chosen, with $CD4^+$ T-cell counts ranging from 70 to 750/mL and HIV-1 RNA ranging from 88 to 150 000 copies per milliliter (Table 1). Two frozen lymph nodes were provided by the National Cancer Institute's AIDS and Cancer Specimen Resource (San Francisco, CA). Patient UMB00-003 had a $CD4^+$ T-cell count of 481/mL 4 months before surgery; patient GW97-91 had a $CD4^+$ T-cell count of 313/mL 9 days before surgery.

Preparation of primary HIV-1 isolate

The HIV-1–infected subject was a naive patient presenting a $CD4^+$ T-cell count of 350/mL and 420 000 HIV-1 RNA copies per milliliter. Two days after HIV-1–infected PBMC isolation, MT4 cells were added to the culture at a concentration of 5×10^5/mL. After 4 more days, supernatants were collected and viral titer was evaluated by a commercial assay (Roche, Basel, Switzerland). U937 cells (5×10^5) were incubated with viral (1.5×10^6 HIV-1 RNA copies per milliliter) or control supernatants for 3 hours at 37°C, washed, and cultured as described.[26]

Preparation of U937/Tat cells

The coding region of *Tat*$_{86}$ from HIV-1 III B was amplified by polymerase chain reaction (PCR) and subcloned into the retroviral vector PINCO [27] under control of the long terminal repeat (LTR) promoter (PINCO/Tat). Phoenix cells were transfected with either the PINCO or PINCO/Tat constructs, and supernatants were used to infect U937 cells. U937/PINCO or U937/Tat cells were isolated either by limit dilution (clonal lines) or by sorting (U937/Tat) with a cell sorter (FACSort Plus; BD Immunocytometry Systems, San Jose, CA).

Transduction with HIV-1–derived lentiviral vectors (LVs)

Vector stocks were prepared by transient cotransfection of 293T cells with the following plasmid combinations: pRRL.hPGK.GFP.SIN-18 + pCMV.ΔR8.2 + pMD.G [28] (VSV-G–LVs) or $pEnv_{HXB}$ [29] (gp120-LVs); pRRL.hPGK.GFP.SIN-18 + pMDLg/pRRE + pRSV-Rev [30] + $pEnv_{HXB}$ (Tat-negative/gp120-LVs). The 293T cell supernatants were used to transduce 10^5 C8166 cells per well of a 48-well plate in the presence of 8 μg/mL polybrene. The input of each kind of lentiviral vector (LV) was normalized to obtain comparable numbers of transduced cells, which were analyzed by cytofluorimetric analysis after 72 hours (FACSCalibur; BD Immunocytometry Systems).

Infection with wild-type, laboratory-adapted HIV-1

Phytohemagglutinin (PHA)–stimulated PBMCs were infected with either HIV-1 III B or Ba-L for 2 hours at 37°C. For evaluation of virus entry, samples were processed as described,[31] with slight modifications. Briefly, cells were lysed in 200 μL of 10 mM Tris (tris(hydroxymethyl)aminomethane)–HCl buffer (pH 8.3) containing 50 mM KCl, 2.5 mM $MgCl_2$, 0.1 mg/mL gelatin, 0.45% Nonidet P-40, 0.45% Tween 20, and 100 μg/mL proteinase K. After protein digestion (2 hours at 56°C) and inactivation of the proteinase (10 minutes at 95°C), 0.1 μL cell lysate was subjected to 35 cycles of PCR using the AmpliTaq Gold system (Perkin Elmer, Shelton, CT), with an annealing temperature of 58°C. Amplified DNA was analyzed by Southern blot hybridization with a ^{32}P-labeled probe and quantified by densitometry with Phoretix 1D (Nonlinear Dynamics, Durham, NC). The following primers and probe were used: R/U5, sense primer 5′-GGCTAACTAGGGAACCCACTG-3′, R/U5 antisense primer 5′-CTGCTAGAGATTTTCCACACTGAC-3′, R/U5 probe 5′-TGTGTGCCCGTCTGTTGTGTG-3′; glyceraldehyde-3-phosphate dehydrogenase (GAPDH) sense primer 5′-ACCACAGTCCATGCCATCAC-3′, GAPDH antisense primer 5′-TCCACCACCCTGTTGCTGTAG-3′.

For evaluation of virus propagation, HIV-1 retrotranscriptase (RT) activity in the cell supernatants was quantified with a standard assay as described.[31]

Quantification of Tat in cell supernatants

Tat concentration in supernatants of HIV-1–infected PBMCs was evaluated by enzyme-linked immunosorbent assay (ELISA) as described.[32] Briefly, 1 μg NT3 2D1 IgG_1 mAb was coated per well of a 96-well plate (Costar, Corning, NY) to immunocapture extracellular Tat, which was then stained with Sp2/0 IgM mAb. This sandwich was incubated with a secondary anti–mouse IgM horseradish peroxidase (HRP)–conjugated Ab (Southern Biotechnology Associates, Birmingham, AL) and quantified using the 1-Step Turbo TMB-ELISA kit (Pierce, Bonn, Germany). Different amounts of rTat were used to draw a standard curve. By this assay, Tat could be quantified in a range of concentrations between 50 pM and 2.5 nM.

Cocultures and incubations with Tat proteins, anti-Tat mAb, and gp120-like peptides

C8166 cells (10^6/mL) were cocultured with HIV-1–infected or control U937 cells and with U937/PINCO or U937/Tat cells in 6-well transwells for 4 hours (unless differently specified) at 37°C or incubated in culture medium containing 7 nM (unless differently specified) of the described Tat proteins for 15 minutes at 37°C. When indicated, cells were treated with NT3 2D1 anti-Tat mAb at a concentration of 10 μg/mL. After treatments, cells were extensively washed in phosphate-buffered saline (PBS) to completely remove unbound Tat and subjected to immunostaining or transduction with LVs. PHA-stimulated PBMCs were incubated with 7 nM rTat for 15 minutes at 37°C, extensively washed, and infected with HIV-1. When indicated, CT303, CT304, CT319, or control peptides were incubated with the cell suspensions at the described concentrations, immediately before adding either LVs or HIV-1.

Immunofluorescence

Cells were prefixed in 0.1% paraformaldeyde in PBS, pH 7.4, for 15 minutes on ice, followed by staining with NT3 2D1 anti-Tat mAb detected by an anti-IgG_1 tetramethylrhodamine isothiocyanate (TRITC)– or phycoerythrin (PE)–conjugated secondary Ab (Southern Biotechnology Associates) and with CRA3 anti-gp120 mAb detected by an anti-IgG_{2a} fluorescein isothiocyanate (FITC)–conjugated secondary Ab (Southern Biotechnology Associates). Analyses of surface-bound Tat were set up using either uninfected PBMCs or untreated C8166 cells as negative controls and

rTat-treated cells as a positive control. Analyses of surface-bound LV and HIV-1 were set up incubating C8166 cells with different amounts of gp120-LVs; 5 μm tissue slides were fixed with 3% paraformaldeyde and stained with the same Abs. Samples were either photographed with a Leica DMIRB inverted microscope equipped with a 40×/0.55 objective lens (Leica Microsystems, Wetzlar, Germany) or analyzed by a cytofluorimeter (FACSCalibur; BD Immunocytometry Systems). For microscopy analysis, cells were spotted onto glass slides and mounted in DakoCytomation Mounting Medium (DakoCytomation, Milan, Italy). Images were captured at room temperature. Photos were acquired through a Hamamatsu c4742-95 camera (Hamamatsu, Hertfordshire, United Kingdom) and by using Image-Pro Plus 4.0.0.13 software (Media Cybernetics, Silver Spring, MD).

Surface-plasmon resonance (SPR) analysis

Evaluation of Tat-gp120 interaction was performed by using a surface-plasmon resonance (SPR)–based BIAcoreX biosensor (BIAcore, Uppsala, Sweden). The rTat was diluted in 5 mM maleate, pH 6.0, and amine-conjugated to a dextran matrix on a CM5 sensor chip surface (BIAcore). Binding of recombinant gp120 (rgp120) was determined over a range of concentrations (1.25 to 50 nM) in 10 mM HEPES (*N*-2-hydroxyethylpiperazine-*N*′-2-ethanesulfonic acid) buffer, pH 7.4, containing 150 mM NaCl, 3 mM EDTA (ethylenediaminetetraacetic acid), 0.005% (vol/vol) polysorbate 20 (HBS-EP buffer; BIAcore) with a flow rate of 5 μL/min at 25°C. Kinetic analysis was performed with the BIAevaluation 3.0.2 software (BIAcore).

Phage display

A total of 10^{10} transducing units (TUs) of either a $CX_{10}C$ or $CX_3CX_3CX_3C$ (C, cysteine; X, any amino acid residue) phage library was added to 10^6 U937/Tat cells in binding medium (20 mM HEPES, pH 7.4, 2% FCS in DMEM) and incubated overnight (first round) or for 2 hours (successive rounds) at 4°C. Cells were washed 5 times with binding medium, and bound phages were recovered and amplified by infection of K91 Kan *Escherichia coli* bacteria at log phase. Purification of phage particles and DNA sequencing of phage-displayed inserts were performed as described.[33-35] Phage binding to rTat-coated microwells was performed with a 10^9 TU input of each phage clone.

Binding assays

One microgram of rgp120 was coated per well of a 96-well plate overnight in PBS. After blocking with 1% bovine serum albumin (BSA) in PBS, the wells were incubated in 0.1% BSA in PBS with the described GST-Tat fusion proteins, and the synthetic peptides when indicated, at a concentration of 7 nM for 1 hour at room temperature. Bound Tat was stained with an anti-GST mAb (Santa Cruz Biotechnology, Santa Cruz, CA) detected by a secondary anti–mouse HRP–conjugated mAb and quantified using the 1-Step Turbo TMB-ELISA kit (Pierce). For experiments performed in the presence of CT304, a logarithmic regression curve has been drawn with Microsoft Excel program and values for 50% inhibitory concentration (IC_{50}) deduced from the x-axis interception.

Statistical analysis

One-way analysis of variance and the Student-Newman-Keuls test were used to test the difference within the blocks of each experiment (STATISTICA 4.5; StatSoft, Tulsa, OK).

Results

Tat is released by HIV-1–infected cells and binds to cell surfaces both in vitro and in vivo

To investigate the presence and localization of Tat in the context of an HIV-1 infection in vitro, we infected peripheral blood mononuclear cells (PBMCs) from healthy donors with 2 laboratory-adapted HIV-1 stains, III B (CXCR4 dependent) and Ba-L (CCR5 dependent). Infection was monitored as RT activity in cell supernatants (Figure 1A). We assessed by ELISA[32] that PBMCs acutely infected by both HIV-1 strains released similar amounts of Tat, ranging from 50 to 250 pM (Figure 1A). Tat was also present on PBMC surfaces, as evaluated by immunostaining and cytofluorimetric analysis. At the peak of infection about 2% of the cells had detectable Tat staining (Figure 1A). We next asked whether cell surface–bound Tat was a biologic feature in HIV-1 pathogenesis (ie, whether our in vitro model could correctly reproduce the situation of infected patients in vivo). We evaluated the presence of Tat on the surfaces of PBMCs from 20 HIV-1–positive patients naive for antiretroviral therapy (ART) (Table 1). By cytofluorimetric analysis we confirmed that up to 6% of cells from 15 patients had detectable amounts of Tat on their surfaces.

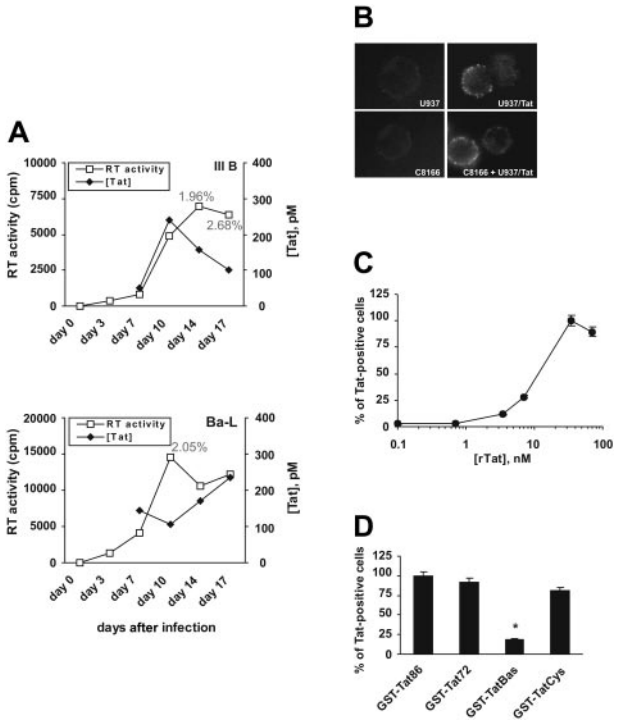

Figure 1. Tat is released by HIV-1–infected cells and binds the cell surface of producing and nearby cells. (A) PBMCs were acutely infected with either III B or Ba-L HIV-1 strains, and Tat amounts (◆) were evaluated both in culture supernatants (by ELISA) and on the cell surfaces (by immunostaining and cytofluorimetric analysis). Numbers represent percent of Tat-positive cells at the indicated time points. The infection was followed for 17 days and monitored as RT activity in the cell supernatants (□). An experiment is shown as representative of 3 performed with comparable results. (B) Anti-Tat NT3 2D1 surface staining of U937/Tat cells and of C8166 cells after coculture with U937/Tat cells. U937/PINCO and C8166 cells are shown as negative controls. These stainings are representative of 3 experiments with similar results. (C) Cytofluorimetric evaluation of rTat binding to the surface of C8166 cells, shown as percent of Tat-positive cells. (D) Identification of Tat region(s) involved in binding the cell surface. C8166 cells were incubated with the described GST-Tat variants, and the amount of Tat-positive cells was detected by cytofluorimetric analysis using an anti-GST mAb. (*$P \leq .01$ versus binding of GST-Tat_{86}). In panels C and D, each value indicates mean ± SD of 2 experiments performed in triplicate.

These results demonstrate that Tat is released by HIV-1–infected cells and is detectable on the cell surfaces both in vitro and in vivo.

HIV-1 Tat localizes at the surface of both Tat-producing and neighboring cells

To further investigate Tat localization, we set up a model mimicking the release of Tat by HIV-1–infected cells. We transduced U937 promonocytic cells with the vector PINCO [27] carrying the Tat_{86}

Table 1. Immunologic and virologic parameters of HIV-1–infected patients for Tat-gp120 analysis

Patient identification	Date	CD4+ T cells per mm3	RNA copies per mL	% Tat-positive cells
KOJE	10/07/1999	73	154274	2.82
NTID	05/20/1998	183	45920	6.15
SAST	11/12/1998	209	5400	1.10
ZULO	06/19/2001	213	135108	1.66
POBRU	10/13/2000	251	63385	0.00
PAMI	06/30/1999	258	6688	2.73
ZULO	06/17/1999	266	69344	2.44
BRARO	05/20/1999	291	50241	3.00
SAPI	01/12/1999	306	5495	2.97
BASE	05/19/1999	403	19029	1.00
TAMA	01/22/1998	408	28973	0.00
ARRA	10/25/1999	423	88	1.00
VERE	06/14/1999	425	2158	1.82
SCHIGI	12/10/1998	440	55000	0.00
MAIS	01/23/2002	484	773	1.37
AROM	10/25/1999	494	13147	1.34
PEAN	11/20/2000	543	1093	0.00
STEP	06/30/1999	588	88	3.22
VEBE	09/30/1999	728	4411	2.00
BALS	07/11/2002	742	42185	0.00

gene of HIV-1 III B. We isolated a cell pool (U937/Tat cells) and several clones, releasing Tat in concentrations from 1.5 to 5 pmol/10^6 cells, as quantified by ELISA.[32] As assessed for HIV-1–infected PBMCs (Figure 1A and Table 1), an anti-Tat immunoreactivity was localized at the cell surface of U937/Tat cells as well (Figure 1B). We then determined if released Tat could bind to surfaces of nearby untransduced cells by coculturing U937/Tat cells with C8166 T lymphocytes in a transwell system in which only the exchange of soluble factors is allowed. We found that after coculture Tat was indeed detectable on the membranes of C8166 cells (Figure 1B).

To quantify Tat binding to cell surfaces, we added increasing concentrations of rTat to the culture medium of C8166 cells. As evaluated by cytofluorimetric analysis, Tat binding is detectable at 2.5 pmol/10^6 cells and reaches a plateau at about 70 pmol/10^6 cells (Figure 1C). We finally investigated the region(s) of Tat responsible for binding to the cell surface. We produced different variants of Tat from HIV-1 HXB2 as GST fusion proteins. GST-Tat_{86}, GST-Tat_{72}, GST-Tat_{Bas}, and GST-Tat_{Cys} [25] were tested for their ability to bind C8166 cells. We detected comparable Tat surface immunoreactivity for all mutants except for Tat_{Bas} (Figure 1D), suggesting that Tat binds to the surface of C8166 cells through its basic region.

HIV-1–infected cell-released Tat enhances virus entry into surrounding cells

To get insights into the mechanism of a possible Tat-mediated HIV-1 infection, we set up experiments using HIV-1–derived LVs.[28,36] In the LV system, HIV-1 genome has been modified so that *(a)* green fluorescent protein (GFP) is expressed for the detection of transduced cells, and *(b)* complete HIV-1 particles are assembled, but *(c)* they are unable to propagate the infection. Therefore, by using LVs it is possible to evaluate early steps of the infection process. We infected U937 cells with a primary isolate from an ART-naive subject. Next, we evaluated LV entry into C8166 cells after coculture with HIV-1–infected U937 cells in a transwell system. We observed that cocultured C8166 cells were up to 50% more permissive to entry of LVs carrying the gp120 envelope of HIV-1 HXB2 (gp120-LVs).[29] This effect was partially reversed by NT3 2D1 anti-Tat mAb but not by control IgG (Figure 2A). Moreover, the enhancement of gp120-LV entry was significantly higher when the coculture was performed with U937 cells 6 days from primary infection, compared with coculture with U937 cells 3 days after infection (Figure 2A).

These results suggest that HIV-1–infected cell-released Tat is responsible for the increase in gp120-LV entry into target cells.

Membrane-bound Tat enhances cell entry of LVs pseudotyped with HIV-1 gp120

We supposed that extracellular Tat could bind the surfaces of both infected Tat-producing cells and neighboring cells and, in such context, play an active role in HIV-1 infection. To investigate this hypothesis we used U937/Tat cells as an in vitro model. We demonstrated that C8166 cells maintained in coculture with

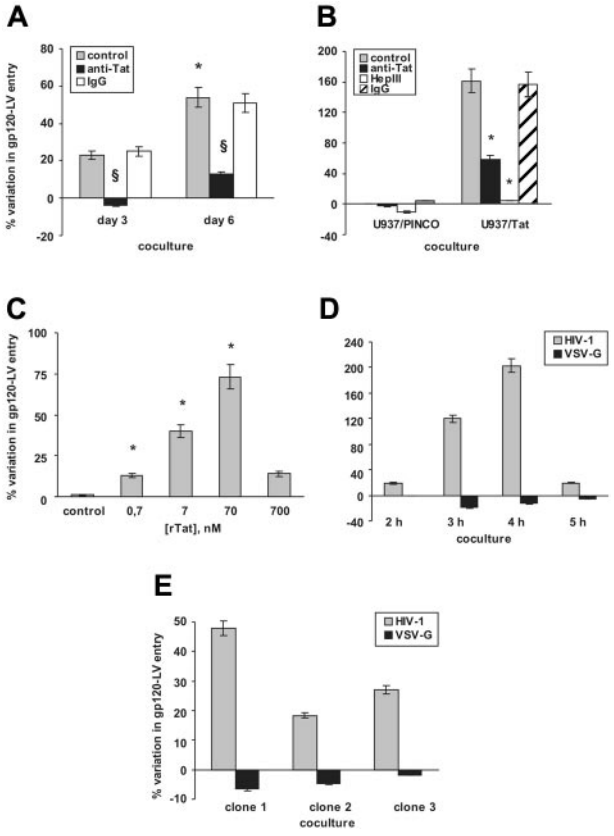

Figure 2. Tat specifically enhances gp120-LV entry. (A) Increase in gp120-LV entry into C8166 cells following coculture with HIV-1–infected U937 cells. During coculture, C8166 cells were either untreated (▨) or pretreated with NT3 2D1 anti-Tat mAb (■) or unrelated IgG (□) as a control (*$P \leq .01$ within day 6 and day 3 after infection; §$P \leq .01$ within anti-Tat–treated and control cells). (B) Increase in gp120-LV entry into C8166 cells following coculture with U937/Tat cells. Cells were either untreated (▨), pretreated with Hep III (□), or incubated with NT3 2D1 anti-Tat mAb (■) or unrelated IgG (▨) as a control (n = 8; F = 624.99; *$P \leq .05$ within treated and control cells). (C) Dose-dependent increase in gp120-LV entry into C8166 cells incubated with rTat (n = 3; F = 258.54; *§$P \leq .05$ within rTat-treated and control cells). (D) Time-course effect of coculture with U937/Tat cells on gp120-LV (HIV-1, ▨) and VSV-G–LV (■) entry into C8166 cells (n = 3; F = 107.4). (E) Effect of 2 hours of coculture with different Tat-expressing clonal lines on gp120-LV and VSV-G–LV entry into C8166 cells (n = 3; F = 937.74). Tat concentrations in these experiments were as follows: U937/Tat, 2.5 nM; clone 1, 5 nM; clone 2, 1.5 nM; clone 3, 3.5 nM. In panels A, B, D, and E, values are shown as percent variation of transduced cells compared with transduction of C8166 cocultured either with uninfected PBMCs or U937/PINCO cells. In panel C, values are shown as percent variation of transduced cells compared with a control transduction of rTat-untreated C8166 cells. Each value indicates mean ± SD of indicated number of experiments performed at least in duplicate.

U937/Tat cells showed an approximate 160% variation in entry of gp120-LVs (Figure 2B). As for the coculture with HIV-1–infected cells, this effect was partially reversed by NT3 2D1 anti-Tat mAb but not by control IgG (Figure 2B). Confirming a role for surface-bound Tat, pretreating the cells with heparinase III (Hep III)—an enzyme that removes sulfate groups from proteoglycans[37]—prevented Tat-driven increase of LV-transduced cells (Figure 2B). To exclude any effect caused by an autocrine activity of Tat on U937/Tat cells, we preincubated C8166 cells with rTat and observed a dose-dependent effect of increasing gp120-LV entry (Figure 2C) that paralleled the numbers of Tat-positive cells (Figure 1C). We then investigated whether Tat-mediated LV entry was influenced by the composition of the viral envelope. For this purpose, we used LVs pseudotyped with vesicular stomatitis virus-G envelope[28] (VSV-G–LVs) for C8166 cell transduction. After coculture with U937/Tat cells for different incubation times (Figure 2D) or with different U937/Tat clonal lines for 2 hours (Figure 2E), we observed that the numbers of VSV-G–LV–transduced cells were not enhanced under any of the experimental conditions tested.

These data demonstrate that the increase in cell entry is strictly dependent not only on surface-bound Tat but also on the presence of an HIV-1 gp120 envelope protein.

Tat is a specific high-affinity ligand of the HIV-1 gp120 envelope protein

We reasoned that Tat and gp120 could interact at the cell surface, thus enhancing gp120-LV entry into cells. To test this hypothesis, we performed SPR analysis to evaluate whether rTat directly interacted with the gp120 protein. BIAcore sensor chips were coated with rTat and exposed to rgp120. A specific binding between these proteins was detected (dissociation constant [K_d] = 8.1 ± 0.3 nM; Figure 3A).

We then mapped the region(s) of gp120 involved in Tat binding by using phage-displayed peptide libraries. Tat-binding peptide motifs were selected after multiple rounds of biopanning on U937/Tat cells. In this system, Tat is concentrated at the cell surface in a conformation that is functionally active in binding the viral envelope. Two different random peptide libraries were used, with the general structures $CX_{10}C$ and $CX_3CX_3CX_3C$ (C, cysteine; X, any amino acid). The libraries were precleared on U937/PINCO cells, and the remaining phages were exposed to U937/Tat cells. Sequencing of the phage isolated after selection revealed 2 peptides that were preferentially enriched, CTVECYFNCTPTC and CPDRKKKVVMVC. Both peptide sequences share homology with a portion of the V1/V2 loop within the gp120 protein, between amino acids (aa) 157 to 171 of gp120 HXB2 (Kuiken et al[38] and Table 2). Tat-binding phages displaying gp120-like peptides were tested for their ability to bind to U937/Tat cells (data not shown) or to rTat-coated microwells. Phage carrying either CTVECYFNCTPTC or CPDRKKKVVMVC peptide specifically bound rTat (Figure 3B), suggesting that these peptides mimic the region of gp120 that interacts with Tat. To further investigate the involvement of gp120 V1/V2 loop in mediating Tat binding, we synthesized soluble peptides designed on a consensus among sequences of the gp120 V1/V2 loops of several HIV-1 strains[38] (peptides CT303 = CSFNIT, CT304 = RDKVKK, and CT319 = CSFNITTEIRDKVKK; see Table 2). We evaluated GST-Tat_{86} binding to rgp120-coated microwells in the presence of increasing peptide concentrations. All the peptides inhibited Tat-gp120 binding, with CT319 showing the highest efficiency (Figure 3C). In these experiments, CT304 showed a complete dose-response effect, while the displacement was not increased by adding concentrations higher than 10 nM and 1 mM for CT319 and CT303, respectively.

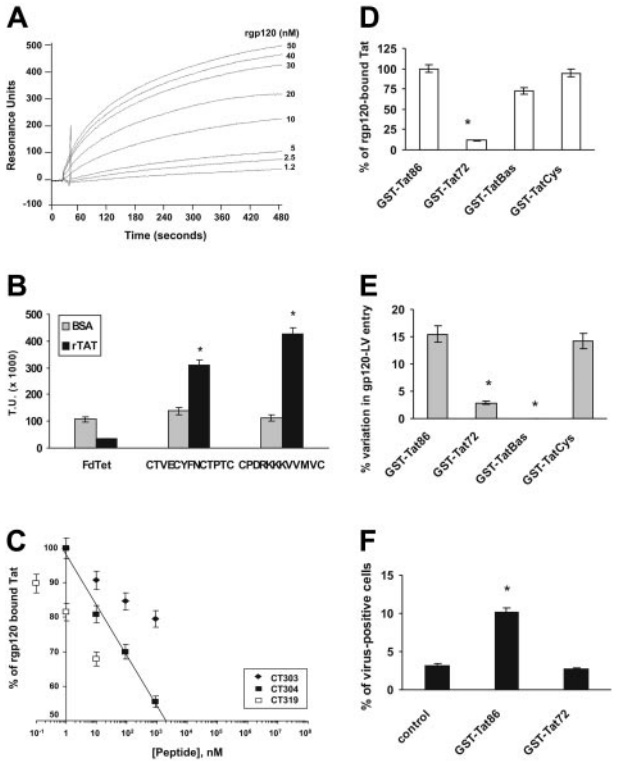

Figure 3. Mapping regions of gp120 and Tat required for their interaction. (A) SPR analysis of Tat-gp120 interaction (n = 3). Recombinant Tat was coated on a sensor chip surface, and binding of rgp120 was evaluated under a range of concentrations (1.25 to 50 nM). (B) Binding of phage display–selected peptide sequences on rTat-coated microwells (■). An insertless phage (FdTet) and BSA (▤) were used as negative controls (n = 6; F = 147.5; * = $P \leq .05$ within rTat- and BSA-coated microwells). (C) Binding of GST-fused Tat_{86} on rgp120-coated microwells in the presence of the gp120-like synthetic peptides (◆, CT303; ■, CT304; □, CT319). GST-Tat_{86} binding in the presence of the control peptide GACVRLSACGA is referred to as 100%. For the CT304 peptide, a logarithmic regression curve has been drawn and values for IC_{50} deduced from the x-axis interception. (D) Binding of GST-fused Tat variants on rgp120-coated microwells. GST-Tat_{86} binding is referred to as 100% (n = 3; F = 76.35; *$P \leq .05$ versus binding to Tat_{86}). (E) Effect of incubation with GST-Tat variants on Tat-negative/gp120-LV entry into C8166 cells (n = 3; F = 233.24; *$P \leq .05$ versus effect of GST-Tat_{86}). Values are shown as percent variation of transduced cells compared with a control transduction of Tat-untreated C8166 cells. (F) Surface-bound Tat enhances virus attachment. Cells were treated with rTat and successively incubated with Tat-negative/gp120-LV. Values are shown as percent of cells with detectable surface staining for Sp2/0 anti-gp120 mAb (n = 3; *$P \leq .03$ versus Tat-negative/gp120-LV binding to Tat-untreated C8166 cells). In B-F, each value indicates mean ± SD of the experiments performed at least in duplicate.

To identify the region(s) of Tat required for gp120 binding, GST-Tat_{86}, GST-Tat_{72}, GST-Tat_{Bas}, and GST-Tat_{Cys} [25] were tested for their ability to bind gp120. All variants except for GST-Tat_{72} bound to rgp120-coated microwells, suggesting that the interaction with gp120 is mediated by Tat aa 73 to 86 (Figure 3D). To reinforce this finding, we evaluated which Tat mutant retained the ability to enhance LV entry into cells. Because Tat protein released by 293T packaging cells might be present in gp120-LV preparations, we produced Tat-deficient,[30] gp120-coated LVs (Tat-negative/gp120-LVs) to completely eliminate any background. We treated C8166 cells with each GST-Tat variant before incubation with Tat-negative/gp120-LVs and found that both GST-Tat_{72} (which does not bind gp120; Figure 3D) and GST-Tat_{Bas} (which does not bind the cell surface; Figure 1D) were unable to enhance Tat-negative/gp120 entry into C8166 cells (Figure 3E). These results suggested that Tat could enhance virus entry by increasing virus attachment to the

Table 2. Phage inserts selected after the third round of panning on U937/Tat cells and sequence alignment of the cognate gp120 regions from different viral strains (derived from Kuiken et al[38])

Phage sequences	
Phage no. 1	CTVE**CYFNCT**PTC
Phage no. 2	CP**DRKKKKV**VHVC
gp120 sequences	
Consensus_A	KNCSFNMTTELRDKKQKVY
Consensus_A1	----------
Consensus_A2	----Y-I-------T----
Consensus_B	------I---I---V--E-
Consensus_C	------I----------
Consensus_D	------I--------KQ-H
Consensus_F1	Q---------V----L--H
Consensus_F2	------I---IK---K-E-
Consensus_G	------I---I----K-E-
Consensus_H	T-----V--VI---Q---H
Consensus_O	-K-E--V--V-K---E-KQ

Bold letters in phage sequences identify the regions with homology to gp120 protein.

surface of host cells. To confirm this hypothesis, we incubated either GST-Tat_{86}– or GST-Tat_{72}–treated C8166 cells with Tat-negative/gp120-LVs in the same conditions as for LV transduction and evaluated the numbers of gp120-positive cells by cytofluorimetric analysis. After incubation with GST-Tat_{86}, about 3 times more cells were positive for gp120 surface staining than in control, untreated cells (Figure 3F). In accordance with the finding that GST-Tat_{72} does not bind to gp120, cells treated with GST-Tat_{72} did not show any increase in gp120 staining (Figure 3F).

These data indicate that the viral envelope protein gp120 specifically interacts through its V1/V2 region with Tat second exon, thus enhancing virus binding and entry into host cells.

Cell surface–bound Tat enhances HIV-1 entry and spreading

To investigate the role of Tat in enhancing HIV-1 infectivity, we designed experiments using PBMCs from healthy donors and 2 HIV-1 strains, III B (CXCR4 dependent) and Ba-L (CCR5 dependent), to control for differences related to viral tropism. We first evaluated if Tat could enhance HIV-1 entry through detection of early viral transcripts in the cytoplasm of infected cells.[31] PBMCs were incubated with rTat, infected with either III B or Ba-L HIV-1, and lysed 2 hours later. We observed increased amounts of early HIV-1 transcripts in the cytoplasm of Tat-treated PBMCs compared with untreated PBMCs regardless of virus strain (Figure 4A). Next, we asked whether Tat-mediated increase of HIV-1 entry could be a crucial step in virus spreading. To answer this question, we followed PBMC infection along 21 days as HIV-1 RT activity in cell supernatants. The rTat-treated PBMCs showed an early peak of Ba-L HIV-1 production, which at day 6 was up to 10-fold higher than in control infections (Figure 4B). Similar results were obtained with III B HIV-1 (data not shown).

These in vitro data suggest that Tat amplifies the spreading of HIV-1 infection in PBMCs by enhancing virus entry into host cells.

In vivo, Tat is detectable on the surfaces of both gp120-negative and gp120-positive cells

To confirm that the described interaction possibly represents a physiological mechanism in the spreading of HIV-1, we evaluated the presence of Tat and gp120 on biologic specimens from HIV-1–infected, ART-naive patients. Five PBMC samples (ARRA, BALS, BRARO, KOJE, and VEBE; see Table 1) and 2 lymph node

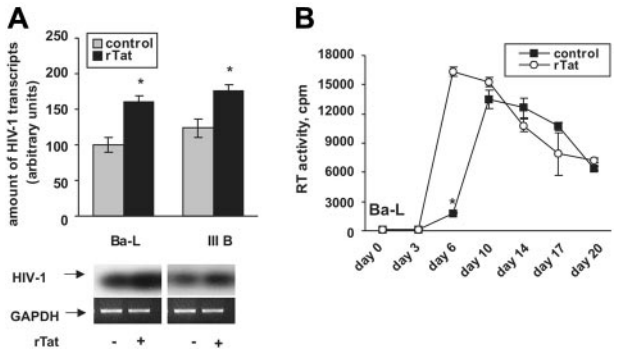

Figure 4. Tat enhances HIV-1 entry and spreading. (A) Tat enhances entry of both CXCR4-dependent HIV-1 strain III B and CCR5-dependent HIV-1 strain Ba-L. PBMCs were either untreated (▤) or pretreated with rTat (■) and immediately infected with either III B or Ba-L. Virus entry was evaluated by a densitometric analysis of the amount of early viral transcripts in the cytoplasm. Tat-mediated increases of III B and Ba-L entry were semiquantitatively corrected by the cognate GAPDH values and expressed as percent of respective control infections. (B) Tat enhances virus spreading in vitro. The amount of HIV-1 produced by infected cells was measured as RT activity in culture supernatants ($F = 165.1$; $^*P \leq .005$ within rTat-treated and control cells). ○ indicates treatment with rTat; ■, control. Similar results were obtained with III B HIV-1 strain. Each value indicates mean ± SD of 3 experiments performed in duplicate.

biopsies (UMB00-003 and GW97-91; see "Materials and methods") were simultaneously stained with NT3 2D1 anti-Tat and CRA3 anti-gp120 mAbs. In both infected compartments we observed 3 different populations: *(a)* Tat-positive cells, *(b)* gp120-positive cells, and *(c)* cells positive for both antigens, with region of possible colocalization (Figure 5; results of Tat staining on samples BALS, BRARO, and VEBE are also shown in Table 1). These results demonstrate that in specimens from HIV-1–positive patients *(a)* cells with no detectable staining for gp120 may be covered by Tat, thus representing potential targets for enhanced HIV-1 infection, and *(b)* Tat and gp120 could be simultaneously present on the cell surface, suggesting that they could interact in vivo.

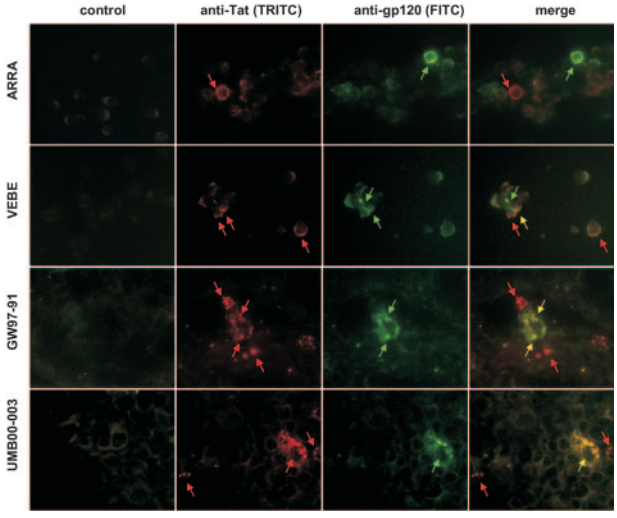

Figure 5. Tat is detectable on the surfaces of both gp120-positive and gp120-negative cells in vivo. Two PBMC samples (ARRA and VEBE) and 2 lymph node biopsies (UMB00-003 and GW97-91) were simultaneously stained with NT3 2D1 IgG_1 anti-Tat and CRA3 IgG_{2a} anti-gp120 antibodies, followed by detection with anti-IgG_1–TRITC and anti-IgG_{2a}–FITC secondary antibodies. Arrows point at specific staining either for Tat (red), gp120 (green), or colocalization of the 2 proteins (yellow). Control pictures are staining with secondary Ab only.

Glycoprotein 120–mimic peptides revert Tat-driven HIV-1 entry and spreading

Finally, we evaluated whether synthetic gp120-mimic peptides could block Tat-mediated HIV-1 infection. We first investigated if the gp120-mimic peptides could block virus entry. We incubated the peptides with C8166 cells at increasing concentrations; in accordance with Tat-gp120 displacement shown in Figure 3C, we chose incubations ranging from 10 to 100 μM for CT303 and CT304 and from 10 nM to 1 μM for CT319. An unrelated peptide (GACVRLSACGA) was used as a negative control. For infection experiments, we used supernatants of infected cells in which Tat is already present (Figure 1A). In these experimental conditions, the gp120-mimic peptides specifically inhibited entry of both HIV-1 strains (Figure 6A). We also performed infections after incubation of cells with rTat (Figure 4A); under these conditions, as expected the gp120-mimic peptides exhibited substantially enhanced efficacy in inhibiting infection (similar results were obtained with both viral strains; Figure 6B).

We next investigated the effect of gp120-mimic peptides on the spreading of viral infection. The rTat-treated PBMCs were infected in presence of CT319 peptide, which completely abolished rTat-driven virus propagation at a concentration as low as 1 nM (Figure 6C; compare with Figure 4B). We also evaluated the efficacy of CT319 to inhibit endogenous Tat-mediated HIV-1 infection. For this purpose, we added the peptide to infected PBMCs every 72 hours either at 1 or 10 nM concentration. Both III B and Ba-L production was inhibited by CT319 (Figure 6D), with a marked inhibitory effect detectable after 6 to 10 days after primary infection, by which time Tat is released into the culture medium and binds the cell surface (Figure 1A). To confirm the specificity of this inhibition, we performed infections in which CT319 was added as a single administration at different time points after primary infection. With an administration at day 7 the infection was delayed, at day 10 it was inhibited, and at day 14 (peak of surface-bound Tat; Figure 1A) it was completely blocked (Figure 6E).

These results demonstrate that Tat-driven infection is specifically reverted by a gp120-mimic peptide that possibly interferes with Tat-gp120 interaction at the cell surface.

Discussion

Our results provide evidence for a novel mechanism of HIV-1 entry, which could be a new therapeutic target to control infection and spreading of the virus.

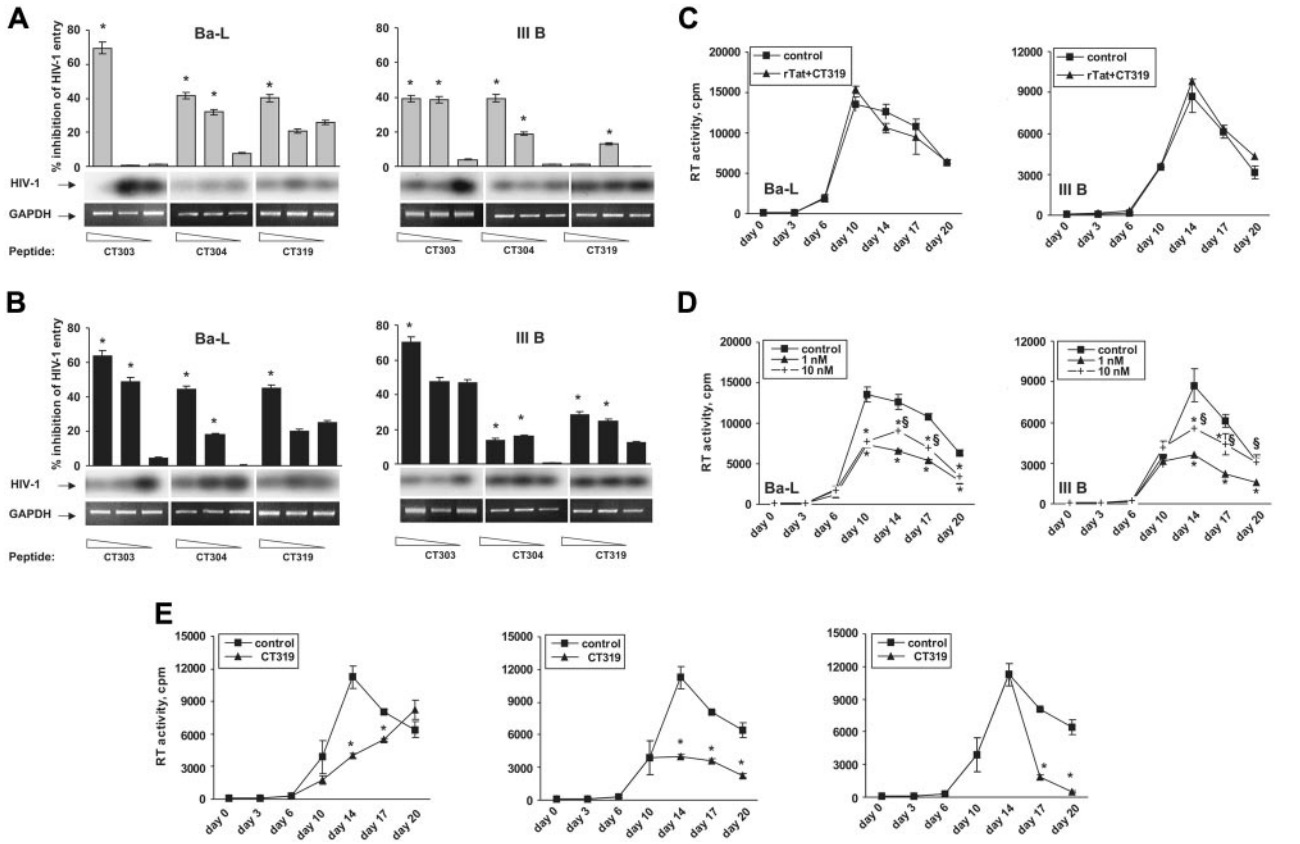

Figure 6. Glycoprotein 120–mimic peptides inhibit HIV-1 entry and spreading. (A) Inhibition of basal infection by gp120-mimic peptides. PBMCs were infected with either III B ($F = 268.78$; $^*P \leq .05$ versus the lowest concentration of each peptide) or Ba-L ($F = 175.54$; $^*P \leq .05$). (B) Inhibition of Tat-promoted infection by gp120-mimic peptides. PBMCs were treated with rTat and infected with III B ($F = 156.73$; $P \leq .05$) or Ba-L ($F = 160.73$; $P \leq .05$). In panels A and B, percent inhibition of virus entry was evaluated as described in the legend to Figure 4A, compared with respective control infections; peptide concentrations were as follows: CT303 and CT304, 100 to 50 to 10 μM; CT319, 1 μM to 100 to 10 nM. (C) CT319 reverts Tat-induced spreading of the infection. PBMCs were infected with either III B or Ba-L in presence of rTat (as shown in Figure 4) and 1 nM CT319 (▲) or GACVRLSACGA control peptide (■). (D) CT319 exhibits a dose-dependent inhibitory effect on HIV-1 spreading. PBMCs were infected with III B or Ba-L and treated every 72 hours with the indicated amounts of CT319 (▲, 1 nM; +, 10 nM) or with 10 nM GACVRLSACGA control peptide (■; III B, $F = 124.3$; Ba-L, $F = 418.6$; $^*P \leq .005$ within CT319-treated and control cells, §$P \leq .005$ versus the lowest peptide concentration tested). (E) Single peptide administrations have different outcomes on the spreading of the infection. PBMCs were infected with III B, and 1 nM CT319 (▲) or GACVRLSACGA control peptide (■) was administered at the indicated time points (III B, $F = 219.8$; Ba-L, $F = 818.2$; $^*P \leq .005$ within CT319-treated and control cells). Similar results were obtained for Ba-L infection. Each value indicates mean ± SD of 3 experiments performed in triplicate.

We started from the observation that HIV-1–infected cells promote virus entry into nearby cells (Figure 2A). This effect is mediated by infected cell-released Tat and is consistent with Tat production observed in vitro in the onset of an acute infection (Figure 1A). We show that extracellular Tat is concentrated on the surfaces of both HIV-1–infected and surrounding uninfected cells both in vitro and in vivo (Figure 1 and Table 1). We hypothesized that the cell surface could function as a reservoir for Tat, which, in that context, could enhance virus entry. This hypothesis first arose from the observation that the basic domain of Tat is responsible for its uptake by cells[39,40]; this property has been used to promote intracellular delivery of nucleic acids[41,42] and proteins[43,44] both in vitro and in vivo. In those experiments, Tat either interacted electrostatically with nucleic acids or was fused to proteins; those unspecific interactions required high Tat amounts (micromolar range). Similar concentrations of Tat (100 μM) are necessary to facilitate cell entry of adenoviral vectors.[45] Recently, Tat amounts that could be reached in HIV-1–infected lymphoid tissues (0.167 μM) have been shown to enhance Kaposi sarcoma–associated herpesvirus (KSHV) infectivity.[46]

Our results provide evidence that Tat-driven enhancement of HIV-1 entry is a consequence of specific interactions between Tat and gp120 at the cell surface (Figure 3). Interestingly, rTat enhances LV entry of 50% at a 7 nM concentration, close to the K_d value for Tat-gp120 binding, as evaluated by SPR analysis (K_d about 8 nM; Figure 3A). The peak of Tat-induced enhancement of LV-transduced cells is reached at 70 nM (Figure 2C), which is 10- to 100-fold higher than Tat amounts detected in infected sera.[9] However, heparan sulfate proteoglycans sequester and concentrate Tat at the cell surface,[8,37] making it possible to obtain high local concentration of Tat both in vitro and in vivo (Figure 1 and Table 1). Moreover, in lymphoid tissue, viral load and Tat amounts go beyond by orders of magnitude than in bloodstream.[47,48]

Our results also indicate that Tat-mediated enhancement of LV-transduced cells is independent from its transactivating activity. First, we observed that Tat concentrations and incubation times not sufficient to involve genes transcriptionally modulated by Tat[49] were optimal to increase virus entry (Figure 2C). On the contrary, cells that were exposed to higher doses of Tat (Figure 2C) or incubated for longer periods of time (Figure 2D) were not efficiently transduced by gp120-LVs. Tat-mediated induction of apoptosis could explain this observation.[9,50] Alternatively, one could reason that an interaction with the HIV-1 coreceptor CXCR4 could lead to inhibition of LV entry.[51-53] Furthermore, the fact that Tat is not able to enhance the numbers of VSV-G–LV–transduced cells excludes any unspecific postentry effect on LV integration and/or on GFP production (Figure 2D-E).

We demonstrate that the regions involved in Tat-gp120 interaction are the V1/V2 loop of the envelope protein (by means of phage-displayed peptide libraries) and the second exon of Tat (by means of GST-fused Tat mutants) (Figure 3). The V1/V2 loop is exposed in the context of the protein structure, suggesting that this is a site that could interact with viral receptors. However, this region is not directly involved in binding the HIV-1 receptor CD4 or coreceptors such as CCR5 and CXCR4.[54-56] Moreover, despite the high variability of the V1/V2 loop, the portion mapped by the phage display–selected peptides is conserved, particularly the "C-S/T/E-F-basic-apolar-S/T" and the "R/K-D/N-basic stretch" motifs (Kuiken et al[38] and Table 2), suggesting a functional role for this region. For what concerns Tat, we found that both the second exon and the basic domain are necessary for enhancing LV entry; although retaining the ability to bind gp120, GST-Tat_{Bas} was ineffective at being unable to bind the cell surface (Figure 1D). In the experiments with Tat recombinant proteins, we used the 86-aa Tat from the laboratory-adapted HIV-1 strains III B (rTat) and HXB2 (GST-fused Tat variants); sequence alignments show that this region is strongly conserved also in 101-aa Tat proteins from HIV-1 wild-type strains (Table 3), suggesting that aa 87 to 101 may be dispensable for the described mechanism. Intriguingly, 7 of 15 aa are identical or homologous also in Tat proteins from different HIV-2 strains (Table 3); on the basis of these homologies, one could speculate Tat-mediated enhancement of virus entry could be possible also for HIV-2 infection.

Table 3. Alignment of Tat sequences (the first 15 aa of the second exon, corresponding to aa 73 to 86 of Tat from HXB2/III B HIV-1) from different HIV-1 and HIV-2 strains

HIV-1, laboratory-adapted	
III B	QPTSQSRGDPTGPKE
HXB2	-----P---------
HIV-1, wild type	
Consensus_A1	--IP-TQ-VS---E-
Consensus_A2	-SLP-TQRVS---E-
Consensus_B	--A--P---------
Consensus_C	--LP-T------SE-
Consensus_D	--S--P---------
Consensus_F1	--L--A--N------
Consensus_F2	--L--T-------E-
Consensus_G	--LPTT--N----E-
Consensus_H	--L-RT---------
Consensus_O	--SI-T-RKQKRQE-
HIV-2, wild type	
Consensus_H2A	KSI-TRT--SQPT-Q
Consensus_H2B	KSL-ART--SQPT-K
H2AB	KSV-TRTRNSQPT-K
H2G	NESISAT-NXQPK--
Consensus_MAC	K-I-NRT-HCQPE-A
Consensus_SMM	KSL-RRA-NCQPK-K
Conserved HIV-1/HIV-2	*** *** *

*Amino acidic residues present in strains of both kinds of viruses (sequences derived from Kuiken et al[38]).

A previously published work[57] shows data both in agreement and in apparent contrast with our results, which need discussion. Tat-mediated effects are various and complex, but for the present discussion one could assume that it has 2 roles in virus propagation: entry (enhanced infection) and transactivation (production of new viral particles). In the cited paper, a role for Tat second exon in viral replication is suggested by the delayed growth kinetic of mutated viruses expressing only Tat first exon. One may speculate that this effect is due to the absence of Tat-mediated virus entry, only basal entry plus transactivation being effective. With a specular experiment, we show an earlier peak of virus replication by treating cells with rTat immediately before the infection (Figure 4). In this case, the effect is due to basal virus entry plus transactivation plus Tat-mediated virus entry.

The proportion of Tat-mediated virus entry seems to be strictly dependent on the cell type. This is an interesting issue that could be related to the number or the availability of receptors on the cell surfaces as well as to other so far unknown players in the complex system of virus/cell recognition and infection. Interestingly, as described by Neuveut and Jeang,[57] infection of PBMCs is almost completely blocked in absence of Tat second exon. Such a result, obtained with transactivation-competent Tat first exon variants, might suggest Tat-mediated virus entry to be of pivotal importance in primary cells (ie, in these cells transactivation is not sufficient to sustain virus growth due to an inefficient basal entry). This raises

an intriguing speculation: primary cells lack a molecular adjuvant of virus entry in the absence of Tat, or they have a molecular block that does not allow entry in basal conditions. This means that Tat may use different molecules instead of or together with HIV-1 classical receptors. We are currently investigating this point.

In the cited paper,[57] the authors describe several mutants of both first exon and full-length Tat, whose behavior could somehow contrast with our results. Four mutants of full-length Tat have mutations in the first exon that do not influence or just slightly modify transactivation; however, those mutants show either a complete absence or a delay of replication. These results involve Tat first exon in transactivation-independent viral replication. One can speculate that *(1)* some mutations in the first exon change Tat 3-dimensional (3D) structure, influencing the availability of the second exon for gp120 binding; *(2)* Tat regions other than the second exon are involved in gp120 binding; and *(3)* Tat first exon is needed for interactions with other known (receptors, coreceptors, surface proteoglycans) or unknown molecular players. Interestingly, a mutation in the region 73 to 86 of the second exon leads to delayed virus proliferation without influencing transactivation, confirming our model. On the other hand, a mutation in a downstream region causes an increase in virus replication without influencing transactivation: this means that aa in the region 87 to 101 (although apparently dispensable for Tat-mediated virus entry) may influence this mechanism, possibly by changing the 3D structure of the 73 to 86 region and/or its affinity for gp120. However, mutations in the second exon appear to be very rare, confirming a pivotal role for this region in virus proliferation.

Despite the huge amount of data on the extracellular effects of Tat and its role in the pathogenesis of HIV-1–associated diseases, the present report demonstrates for the first time a specific role in HIV-1 infectivity. It is well known that HIV-1 infection is mainly dependent on the presence of CD4 and CXCR4/CCR5; we propose that surface-bound Tat could partially enhance HIV-1 entry into host cells (Figures 2 and 4). We also provide evidence that the Tat-gp120 interaction is likely to occur in vivo during viral spreading, as demonstrated by the colocalization of anti-Tat and anti-gp120 staining both on PBMCs and in lymph node biopsies from HIV-1–positive patients (Figure 5). Our experiments show that Tat can enhance the entry of viruses that use either CXCR4 (III B) or CCR5 (Ba-L) as coreceptors (Figure 4A), suggesting a broad-range mechanism for Tat-driven HIV-1 infection. Because virus spreading follows an exponential trend, an increase in HIV-1 entry as low as 60% is sufficient to give a 10-fold increase in virus production after 6 days from primary infection (Figure 4B).

We also investigated the potential use of the phage display–selected peptides as drugs against HIV-1 infection. We observed that these peptides compete with gp120 V1/V2 loop for Tat binding in vitro (Figure 3C) and suggested that they can inhibit this interaction on the cell surface; in accordance with this hypothesis, we observed that the gp120-mimic peptides do not interfere with Tat transactivation activity (S.M., unpublished data, 2003). We observed that both virus entry and propagation are significantly blocked by the gp120-mimic peptides in a Tat-dependent manner; this effect is independent from the viral strain (Figure 6). These results are consistent with the observation that the region of V1/V2 loop involved in Tat binding is quite conserved along different HIV-1 strains.[38] Based on our experimental data, we propose that gp120-like peptidomimetic derivatives could be developed as broad-range anti-AIDS drugs to be used in association with other antiretroviral therapies.

Acknowledgments

We thank G. Poli and L. Naldini for suggestions about HIV-1 and LV infection experiments and M. Montroni and S. Fumero for critical reading of the manuscript. The described peptides and their peptidomimetic derivatives are protected by an international patent application (no. PCT/EP03/10162) and will be developed by Creabilis as potential anti–HIV-1 drugs.

References

1. Coombs RW, Collier AC, Allain JP, et al. Plasma viremia in human immunodeficiency virus infection. N Engl J Med. 1989;321:1626-1631.
2. Fauci AS, Schnittman SM, Poli G, Koenig S, Pantaleo G. NIH conference. Immunopathogenic mechanisms in human immunodeficiency virus (HIV) infection. Ann Intern Med. 1991;114:678-693.
3. Ho DD, Moudgil T, Alam M. Quantitation of human immunodeficiency virus type 1 in the blood of infected persons. N Engl J Med. 1989;321:1621-1625.
4. Blankson JN, Persaud D, Siliciano RF. The challenge of viral reservoirs in HIV-1 infection. Annu Rev Med. 2002;53:557-593.
5. Fauci AS. Host factors and the pathogenesis of HIV-induced disease. Nature. 1996;384:529-534.
6. Marciniak RA, Calnan BJ, Frankel AD, Sharp PA. HIV-1 Tat protein trans-activates transcription in vitro. Cell. 1990;63:791-802.
7. Ensoli B, Barillari G, Salahuddin SZ, Gallo RC, Wong-Staal F. Tat protein of HIV-1 stimulates growth of cells derived from Kaposi's sarcoma lesions of AIDS patients. Nature. 1990;345:84-86.
8. Ensoli B, Buonaguro L, Barillari G, et al. Release, uptake, and effects of extracellular human immunodeficiency virus type 1 Tat protein on cell growth and viral transactivation. J Virol. 1993;67:277-287.
9. Westendorp MO, Frank R, Ochsenbauer C, et al. Sensitization of T cells to CD95-mediated apoptosis by HIV-1 Tat and gp120. Nature. 1995;375:497-500.
10. Albini A, Barillari G, Benelli R, Gallo RC, Ensoli B. Angiogenic properties of human immunodeficiency virus type 1 Tat protein. Proc Natl Acad Sci U S A. 1995;92:4838-4842.
11. Liu Y, Jones M, Hingtgen CM, et al. Uptake of HIV-1 tat protein mediated by low-density lipoprotein receptor-related protein disrupts the neuronal metabolic balance of the receptor ligands. Nat Med. 2000;6:1380-1387.
12. Chirivi RG, Taraboletti G, Bani MR, et al. Human immunodeficiency virus-1 (HIV-1)-Tat protein promotes migration of acquired immunodeficiency syndrome-related lymphoma cells and enhances their adhesion to endothelial cells. Blood. 1999;94:1747-1754.
13. Conaldi PG, Bottelli A, Baj A, et al. Human immunodeficiency virus-1 tat induces hyperproliferation and dysregulation of renal glomerular epithelial cells. Am J Pathol. 2002;161:53-61.
14. Huang LM, Joshi A, Willey R, Orenstein J, Jeang KT. Human immunodeficiency viruses regulated by alternative trans-activators: genetic evidence for a novel non-transcriptional function of Tat in virion infectivity. EMBO J. 1994;13:2886-2896.
15. Smith SM, Penticky S, Klase Z, et al. An in vivo replication-important function in the second coding exon of Tat is constrained against mutation despite cytotoxic T lymphocyte selection. J Biol Chem. 2003;278:44816-44825.
16. Neuveut C, Scoggins R, Camerini D, Markham RB, Jeang KT. Requirement for the second coding exon of Tat in the optimal replication of macrophage-tropic HIV-1. J Biomed Sci. 2003;10:651-660.
17. Re MC, Vignoli M, Furlini G, et al. Antibodies against full-length Tat protein and some low-molecular-weight Tat-peptides correlate with low or undetectable viral load in HIV-1 seropositive patients. J Clin Virol. 2001;21:81-89.
18. Opi S, Peloponese JM Jr, Esquieu D, et al. Tat HIV-1 primary and tertiary structures critical to immune response against non-homologous variants. J Biol Chem. 2002;277:35915-35919.
19. Addo MM, Altfeld M, Rosenberg ES, et al. The HIV-1 regulatory proteins Tat and Rev are frequently targeted by cytotoxic T lymphocytes derived from HIV-1-infected individuals. Proc Natl Acad Sci U S A. 2001;98:1781-1786.
20. Agwale SM, Shata MT, Reitz MS Jr, et al. A Tat subunit vaccine confers protective immunity against the immune-modulating activity of the human immunodeficiency virus type-1 Tat protein in mice. Proc Natl Acad Sci U S A. 2002;99:10037-10041.
21. Cafaro A, Caputo A, Fracasso C, et al. Control of SHIV-89.6P-infection of cynomolgus monkeys by HIV-1 Tat protein vaccine. Nat Med. 1999;5:643-650.

22. Re MC, Gibellini D, Vitone F, La Placa M. Antibody to HIV-1 Tat protein, a key molecule in HIV-1 pathogenesis. A brief review. New Microbiol. 2001;24:197-205.
23. Gallo RC. Tat as one key to HIV-induced immune pathogenesis and Tat (correction of Pat) toxoid as an important component of a vaccine. Proc Natl Acad Sci U S A. 1999;96:8324-8326.
24. Goldstein G. HIV-1 Tat protein as a potential AIDS vaccine. Nat Med. 1996;2:960-964.
25. Mitola S, Soldi R, Zanon I, et al. Identification of specific molecular structures of human immunodeficiency virus type 1 Tat relevant for its biological effects on vascular endothelial cells. J Virol. 2000;74:344-353.
26. Savarino A, Gennero L, Chen HC, et al. Anti-HIV effects of chloroquine: mechanisms of inhibition and spectrum of activity. AIDS. 2001;15:2221-2229.
27. Grignani F, Kinsella T, Mencarelli A, et al. High-efficiency gene transfer and selection of human hematopoietic progenitor cells with a hybrid EBV/retroviral vector expressing the green fluorescence protein. Cancer Res. 1998;58:14-19.
28. Naldini L, Blomer U, Gallay P, et al. In vivo gene delivery and stable transduction of nondividing cells by a lentiviral vector. Science. 1996;272:263-267.
29. Huang L, Bosch I, Hofmann W, Sodroski J, Pardee AB. Tat protein induces human immunodeficiency virus type 1 (HIV-1) coreceptors and promotes infection with both macrophage-tropic and T-lymphotropic HIV-1 strains. J Virol. 1998;72:8952-8960.
30. Dull T, Zufferey R, Kelly M, et al. A third-generation lentivirus vector with a conditional packaging system. J Virol. 1998;72:8463-8471.
31. Schmidtmayerova H, Alfano M, Nuovo G, Bukrinsky M. Human immunodeficiency virus type 1 T-lymphotropic strains enter macrophages via a CD4- and CXCR4-mediated pathway: replication is restricted at a postentry level. J Virol. 1998;72:4633-4642.
32. Hudson L, Liu J, Nath A, et al. Detection of the human immunodeficiency virus regulatory protein tat in CNS tissues. J Neurovirol. 2000;6:145-155.
33. Smith GP, Scott JK. Libraries of peptides and proteins displayed on filamentous phage. Methods Enzymol. 1993;217:228-257.
34. Scott JK, Smith GP. Searching for peptide ligands with an epitope library. Science. 1990;249:386-390.
35. Pasqualini R, Arap W, Rajotte D, Ruoslahti E. In vivo phage display. In: Barbas CF, Burton DR, Scott JK, Silverman GJ, eds. Phage Display: A Laboratory Manual. Cold Spring Harbor, NY: Cold Spring Harbor Laboratory Press; 2000:1-24.
36. Naldini L, Blomer U, Gage FH, Trono D, Verma IM. Efficient transfer, integration, and sustained long-term expression of the transgene in adult rat brains injected with a lentiviral vector. Proc Natl Acad Sci U S A. 1996;93:11382-11388.
37. Tyagi M, Rusnati M, Presta M, Giacca M. Internalization of HIV-1 tat requires cell surface heparan sulfate proteoglycans. J Biol Chem. 2001;276:3254-3261.
38. Kuiken C, Foley B, Freed E, et al, eds. HIV Sequence Compendium 2002. Theoretical Biology and Biophysics Group, Los Alamos National Laboratory. 2002:LA-UR no. 03-3564.
39. Wender PA, Mitchell DJ, Pattabiraman K, Pelkey ET, Steinman L, Rothbard JB. The design, synthesis, and evaluation of molecules that enable or enhance cellular uptake: peptoid molecular transporters. Proc Natl Acad Sci U S A. 2000;97:13003-13008.
40. Ho A, Schwarze SR, Mermelstein SJ, Waksman G, Dowdy SF. Synthetic protein transduction domains: enhanced transduction potential in vitro and in vivo. Cancer Res. 2001;61:474-477.
41. Ignatovich IA, Dizhe EB, Pavlotskaya AV, et al. Complexes of plasmid DNA with basic domain 47-57 of the HIV-1 Tat protein are transferred to mammalian cells by endocytosis-mediated pathways. J Biol Chem. 2003;278:42625-42636.
42. Rudolph C, Plank C, Lausier J, Schillinger U, Muller RH, Rosenecker J. Oligomers of the arginine-rich motif of the HIV-1 TAT protein are capable of transferring plasmid DNA into cells. J Biol Chem. 2003;278:11411-11418.
43. Morris MC, Depollier J, Mery J, Heitz F, Divita G. A peptide carrier for the delivery of biologically active proteins into mammalian cells. Nat Biotechnol. 2001;19:1173-1176.
44. Xia H, Mao Q, Davidson BL. The HIV Tat protein transduction domain improves the biodistribution of beta-glucuronidase expressed from recombinant viral vectors. Nat Biotechnol. 2001;19:640-644.
45. Gratton JP, Yu J, Griffith JW, et al. Cell-permeable peptides improve cellular uptake and therapeutic gene delivery of replication-deficient viruses in cells and in vivo. Nat Med. 2003;9:357-362.
46. Aoki Y, Tosato G. HIV-1 Tat enhances Kaposi sarcoma-associated herpesvirus (KSHV) infectivity. Blood. 2004;104:810-814.
47. Pantaleo G, Graziosi C, Fauci AS. The role of lymphoid organs in the pathogenesis of HIV infection. Semin Immunol. 1993;5:157-163.
48. Embretson J, Zupancic M, Ribas JL, et al. Massive covert infection of helper T lymphocytes and macrophages by HIV during the incubation period of AIDS. Nature. 1993;362:359-362.
49. Thomas CA, Dobkin J, Weinberger OK. TAT-mediated transcellular activation of HIV-1 long terminal repeat directed gene expression by HIV-1-infected peripheral blood mononuclear cells. J Immunol. 1994;153:3831-3839.
50. Li CJ, Friedman DJ, Wang C, Metelev V, Pardee AB. Induction of apoptosis in uninfected lymphocytes by HIV-1 Tat protein. Science. 1995;268:429-431.
51. Albini A, Ferrini S, Benelli R, et al. HIV-1 Tat protein mimicry of chemokines. Proc Natl Acad Sci U S A. 1998;95:13153-13158.
52. Ghezzi S, Noonan DM, Aluigi MG, et al. Inhibition of CXCR4-dependent HIV-1 infection by extracellular HIV-1 Tat. Biochem Biophys Res Commun. 2000;270:992-996.
53. Xiao H, Neuveut C, Tiffany HL, et al. Selective CXCR4 antagonism by Tat: implications for in vivo expansion of coreceptor use by HIV-1. Proc Natl Acad Sci U S A. 2000;97:11466-11471.
54. Rizzuto CD, Wyatt R, Hernandez-Ramos N, et al. A conserved HIV gp120 glycoprotein structure involved in chemokine receptor binding. Science. 1998;280:1949-1953.
55. Kwong PD, Wyatt R, Robinson J, Sweet RW, Sodroski J, Hendrickson WA. Structure of an HIV gp120 envelope glycoprotein in complex with the CD4 receptor and a neutralizing human antibody. Nature. 1998;393:648-659.
56. Wyatt R, Kwong PD, Desjardins E, et al. The antigenic structure of the HIV gp120 envelope glycoprotein. Nature. 1998;393:705-711.
57. Neuveut C, Jeang KT. Recombinant human immunodeficiency virus type 1 genomes with tat unconstrained by overlapping reading frames reveal residues in Tat important for replication in tissue culture. J Virol. 1996;70:5572-5581.